In: Space Science: New Research
Editor: Nick S. Maravell, pp. 141-164
ISBN: 1-60021-005-8

Chapter 5

PALEOSHORELINES AND THE EVOLUTION OF THE LITHOSPHERE OF MARS

Javier Ruiz
Departamento de Geodinámica, Facultad de Ciencias Geológicas,
Universidad Complutense de Madrid, 28040 Madrid, Spain
Rosa Tejero
Departamento de Geodinámica, Facultad de Ciencias Geológicas,
Universidad Complutense de Madrid, 28040 Madrid, Spain
David Gómez-Ortiz
Escuela Superior de Ciencias Experimentales y Técnicas-Área de Geología,
Universidad Rey Juan Carlos, 28933 Móstoles, Madrid, Spain
Valle López
Servicio de Sistemas de Información Geográfica, Instituto Geológico y Minero de
España, Ríos Rosas 23, 28003 Madrid, Spain

Abstract

The existence of features indicative of shorelines of ancient oceans on Mars has been proposed for several authors. In this chapter we revise the topography of possible Martian paleoshorelines, and their consequences for the amount of water infilling ocean basins when water load is considered. We show that a re-evaluation of paleoshorelines is need. For example, the putative Meridiani shoreline could be the same feature as some portions of the Arabia shoreline. Indeed, elevations in the Meridiani shoreline are roughly similar to that of the Arabia shoreline in northeast Arabia, Utopia (not taken into account the Isidis basin), Elysium, and Amazonis regions. This is still far of an equipotential surface, but a paleoshoreline through these regions and the Meridiani shoreline would be better candidate to represent a paleoequipotential surface than the Arabia shoreline *sensu strito*. Moreover, the elevation of the Arabia shoreline in northern Arabia Terra after is intriguingly close to the mean elevation of the Deuteronilus shoreline, and it cannot be discarded a “mixed” Arabia/Deuteronilus shoreline, which would include the Arabia shoreline in northern Arabia Terra, and the Deuteronilus shoreline elsewhere.

If reality of global shorelines is accepted, as increasing evidence suggests, then present-day topographic variations in these features postdate shorelines formation. So, their topographic range should provide information on large-scale vertical movement of the lithosphere, which in turn provides information on the thermal evolution of Mars. We describe the application of thermal isostasy concept to constraint the ancient thermal state of the lithosphere from present-day paleoshoreline topography. For the ~1.1 km total elevation range of the Deuteronilus shoreline, the relative amplitude of heat flow variations (the ratio between maximum and minimum heat flow) is ≤1.6. This value is clearly lower than that presently observed on continental areas on the Earth. If heat flow variations on Mars are currently greatly disappeared, then the obtained heat flow variations upper limits must be mostly related to the paleoshoreline formation time: the present-day elevation range along Deuteronilus shoreline suggests that differences in the thermal state of the lithosphere in regions along this putative paleoshoreline have been relatively small since the feature was formed, and therefore the absence of lithospheric tectonothermal events by the latest ~3 Gyr, at least. If the Deuteronilus shoreline is a combination of portions of several paleoshorelines, then the total elevation range, and the implied heat flow variations, would be lower, and the lithosphere stability higher.

Introduction

A plenty of studies about the characteristics, thermal state, and evolution of the lithosphere of Mars has been previously performed from several lines of work.

On a hand, numerous efforts have focused on the mechanical properties of the lithosphere, which serve to calculate its effective elastic thickness and thermal structure (e.g., Comer et al., 1985; Solomon and Head, 1990; Anderson and Grimm, 1998; Zuber et al., 2000; Nimmo, 2002; McGovern et al., 2002, 2004; McKenzie et al., 2002; Kieffer, 2004; Ruiz et al., 2006), and the topography and geometry or greath faults, and hence the brittle-ductile transition depth (e.g., Schultz and Lin, 2001; Schultz and Watters, 2001; Vidal et al., 2005). These studies inform about the thermal structure and heat flow in the time when the structures were formed.

On the other hand, thermal history models make predictions about the evolution of surface heat flow and lithospheric thickness, or even crustal growth (e.g., Stevenson et al., 1983; Schubert and Spohn, 1990; Schubert et al., 1992; Grasset and Parmentier, 1998; Nimmo and Stevenson, 2000; Choblet and Sotin, 2001; Spohn et al., 2001; Hauck and Phillips, 2002; Breuer and Spohn, 2003). Obviously, results from thermal history models should be consistent with constraints imposed by the studies of the mechanical properties of the lithosphere.

A third line of information about the evolution of the Martian lithosphere is the analysis of present-day topography of features interpreted as paleoshorelines. Indeed, the presence of features indicative of shorelines of ancient oceans on Mars has been proposed (Parker et al., 1989, 1993; Edgett and Parker, 1997; Clifford and Parker, 2001). If reality of global paleoshorelines is accepted, then present-day topographic variations in these features postdate shorelines formation. So, their topographic range should provide information on large-scale vertical movement of the lithosphere, which in turn would provide information on the thermal evolution of Mars (Ruiz, 2003): total elevation differences along paleoshorelines impose constraints to the differences in the evolution of the thermal structure of the lithosphere in shoreline-crossed regions. In fact, it is possible to make an approximate calculation of the amplitude of the ancient heat flow variations necessary to compensate, through thermal isostasy, elevation differences, and transform the paleoshorelines into equipotential surfaces. Like other geological processes could have produced vertical movements, the results so obtained suppose an upper limit.

Diverse efforts have been carried out to test reality of the proposed paleoshorelines. Specifically targeted MOC images have been interpreted as not supporting the shoreline hypothesis (Malin and Edgett, 1999, 2001), although these results have been disputed (Parker et al., 2001; Clifford and Parker, 2001; Fairén et al., 2003). Moreover, recent works using high resolution images have found clear evidences of erosion in places located in putative paleoshorelines (Webb and McGill, 2003; Webb, 2004), which support its formation in relation to coastal processes. The observed present-day Martian topography (Smith et al., 1999, 2001) has also been used to analyze elevations along of the main proposed paleoshorelines, in order to test their chance to represent true paleoshorelines (Head et al., 1998, 1999; Carr and Head, 2003, Webb, 2004). These analyses obtain that the Late Hesperian Deuteronilus shoreline is a viable paleoshoreline, since this feature slightly deviates from an equipotential surface. Otherwise, the putative older and higher-standing Arabia shoreline deviates substantially from an equipotential surface, indicating that it may not be representative of a true shoreline.

The evaluation of possible paleoshorelines through assessment of present-day topography must be made cautiously, because it is not necessarily true that a paleoequipotential surface must fit well a present-day equipotential surface. Lithosphere rebound due to water unloading associated with the disappearance of an ocean with irregularly shaped margins could result in deviations of equipotentiality of up to several hundreds of meters (Leverington et al., 2003; Leverington and Ghent, 2004). Different thermal histories among regions may have appreciably contributed to the deformation of the original large wavelength topography of putative paleoshorelines: variations in Martian heat flow, similar in relative amplitude to those observed in terrestrial continental tectonothermally stable areas, could result in large wavelength elevation differences of kilometric scale through differential thermal isostasy (Ruiz, 2003, Ruiz et al., 2003, 2004), an important amount of deformation for any possible paleoshoreline. Tectonic processes could also produce vertical movements, and erosional or sedimentary activity could affect the original paleoshoreline signatures (Clifford and Parker, 2001). Moreover, lateral continuity of paleoshorelines is not well established, and diverse division and mixing of the originally proposed features are likely required (Ruiz et al, 2003; Webb, 2004; Ruiz, 2005).

In this chapter we revise and re-evaluate the topography of possible Martian paleoshorelines, and the consequences of the water load for the amount of water infilling ocean basins. We also describe the application of thermal isostasy concept to constraint the ancient thermal state of the lithosphere from present-day paleoshoreline topography, and we present the results obtained and their implications for the evolution of the lithosphere of Mars.

Paleoshorelines

In this section we first revise elevation ranges in the paleoshorelines originally proposed by Parker et al. (1989, 1993) and Edgett and Parker (1997), which were revised, redrawn and renamed (as Deuteronilus, Arabia and Meridiani) by Clifford and Parker (2001) (Figure 1 shows a map of Mars with some of the geographical features mentioned in the text, and

Figure 2 shows the paleoshorelines after Clifford and Parker (2001) represented on the Martian topography). Later, we use MOLA topography (Smith et al., 1999, 2001) to refine calculations of the water volume infilling the ancient oceanic basins, by taking into account both present-day topography and the maximum possible effect caused by the water weight on the oceanic floors topography. Finally, we re-evaluate these features through of comparing their respective elevations (geomorphologic revisions or re-evaluations are beyond the scope of this chapter), using the mapping of Clifford and Parker (2001) and MOLA topography.

In this point it is necessary recall that Martian elevations are given with respect to an arbitrary zero elevation level, defined as the equipotential surface (gravitational + rotational) whose average value at the equator is equal to the mean radius (see Smith et al., 2001).

Table 1. Martian chronology after Hartmann and Neukum (2001) and Hartmann (2005).

Period	Age (Gyr)
Late Amazonian	
	0.2-0.6
Middle Amazonian	
	1.4-2.1
Early Amazonian	
	2.9-3.2
Late Hesperian	
	3.2-3.6
Early Hesperian	
	3.5-3.7
Late Noachian	
	3.6-3.9
Middle Noachian	
	3.8-4.1
Early Noachian	

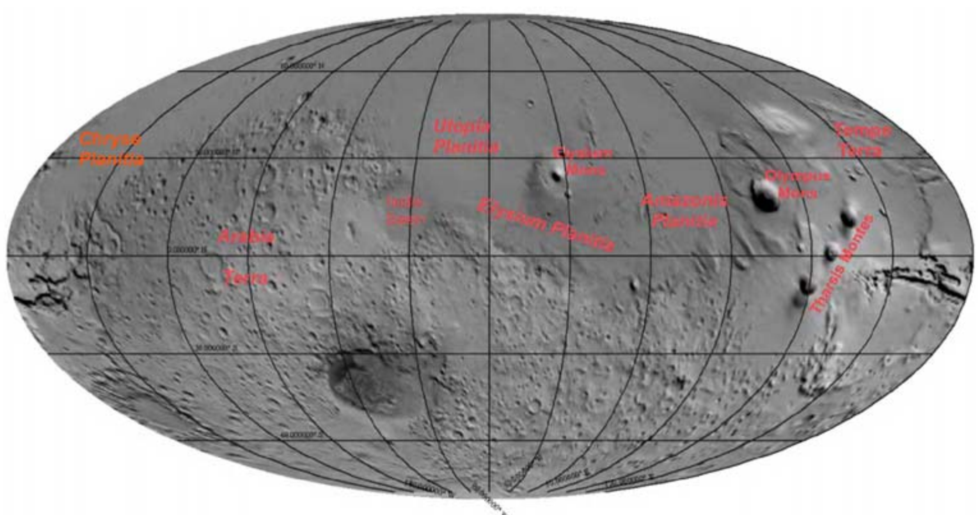

Figure 1. Map of Mars with some of the geographical features mentioned in the text, and other representative features indicated on the Martian topography.

Elevations Range along Deuteronilus, Arabia, and Meridiani Shorelines

The better evidence for a Martian paleoshoreline (dating from the Late Hesperian; temporal equivalences, as obtained from crater counts statistical, are given in Table 1) is the presence in the northern lowlands of a mapping contact (originally named Contact 2) marking the outer boundary of the northern plains, which was interpreted to be the shoreline of an ancient Martian ocean (Parker et al., 1989, 1993). This “contact” was later redrawn and renamed Deuteronilus shoreline by Clifford and Parker (2001). Head et al. (1998, 1999) and Carr and Head (2003), using MOLA data, have shown that this putative shoreline represents a relatively good approximation to an equipotential surface: its mean altitude is −3.792 ± 0.236 km, and its whole topographic range is ~1.1 km, from −3.2 to −4.3 km (Carr and Head, 2003). The elevation of the base levels of the Chryse outflow channels, −3.742 ± 0.153 km (Ivanov and Head, 2001), is close to the mean level of Deuteronilus shoreline, could also indicate that they debouched into a large standing body of water (Head et al., 1999; Ivanov and Head, 2001); this seem also be the case for other channels termini (Salamuniccar, 2004). Additionally, there is clear evidence for erosion along the Deuteronilus shoreline (Webb, 2004).

Alternatively (or complementarily), Carr and Head (2003) considered that the Late Hesperian Vastitas Borealis Formation, which extends for a great part of the northern lowlands, represents better support for the past existence of a large standing body of water on Mars. The Vastitas Borealis Formation has been interpreted as a sedimentary veneer at least 100 m thick on the East Hesperian ridged plains (Head et al., 2002), which could have originated as a sublimation residue from a large (probably frozen) water body (Kreslavsky and Head, 2002). The outer contact of the Vastitas Borealis Formation is coincident with the trace of the Deuteronilus shoreline in the Deuteronilus, Nilosyrtis, Isidis, Tempe, and Chryse regions, but not in Elysium or the Olympus Mons aureole. If the outer contact of the Vastitas Borealis Formation in the Utopia basin is ignored (where it is covered by younger Amazonian Elysium materials, and therefore, the original contact trace is not visible), the outer contact of the Vastitas Borealis Formation has a mean altitude of −3.658 ± 0.282 km, with a whole elevation range of ~1.0 km, from −3.3 to −4.3 km (Carr and Head, 2003; see their Figure 12).

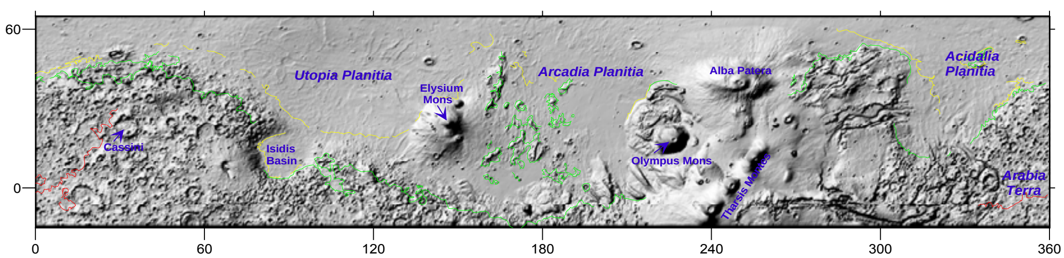

Figure 2. The Deuteronilus (yellow), Arabia (green) and Meridiani (red) shorelines after Clifford and Parker (2001), represented on the Martian topography.

Parker et al. (1989, 1993) also proposed an older, higher-standing Contact 1, later on renamed Arabia shoreline (Clifford and Parker, 2001). This shoreline, which would be of Noachian age (see Clifford and Parker, 2001), is roughly coincident with the Martian dichotomy separating the lowlands from the highlands, and the elevation along its outline highly deviates from an equipotential surface (Head et al., 1998, 1999), and thus it is not a good candidate to paleoshoreline. The topography along the Arabia shoreline is characterized (Carr and Head, 2003) by a mean altitude of −2.090 ± 1.400 km, and a total elevation range of ~5.6 km (from 1.6 to −4.0 km).

Finally, the existence of a pre-Arabia shoreline has been proposed in northern Sinus Meridiani and western Arabia Terra (Edgett and Parker, 1997; Clifford and Parker, 2001); precisely, the MER Opportunity has recently found evidences for an aqueous, maybe sea-related, environment at Meridiani Planum, close to this possible paleoshoreline (Squyres et al., 2004). The mean elevation of this Meridiani shoreline (as named by Clifford and Parker, 2001), would be about −1.5 km (Parker et al., 2000), although its topography has not been examined in previous works. Figure 3 shows constant elevation contours (0.5 km spaced) crossed by the Meridiani shoreline. It can be seen that elevations along the mapped paleoshoreline mostly range between 0 and −2 km. If Hesperian chaos materials (see Tanaka et al., 1992), impact craters, and an isolated peak are not taken into account (see also Figure 6), then total elevation range is ~1 km, from −0.5 to −1.5 km, a reasonable amount for a very old paleoshoreline.

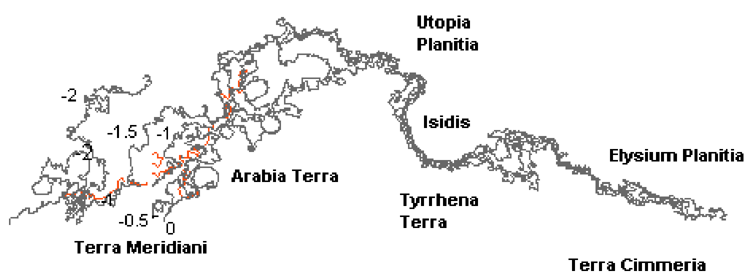

Figure 3. Constant elevation contours in km (black) crossed by the Meridiani shoreline (red). Elevation contours are spaced 0.5 km.

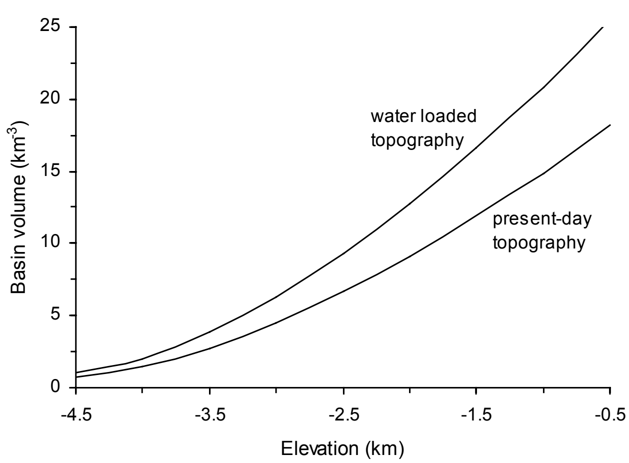

Figure 4. Basin volume as a function of the elevation level, for both, present-day topography and water loaded, Airy compensated, topography (below the -4.35 km level volume includes the contribution from both North Polar and Utopia basins).

Water Volumes in the Ancient Oceans

MOLA topography and mean elevations of proposed paleoshorelines has been previously used to calculate the water volumes contained in the basin related to these putative coastal limits (Head et al., 1998, 1999; Carr and Head, 2003; Öner et al., 2004). Similar calculations are presented in Table 2, and Figure 4 shows basin volume as a function of the elevation level. For the Meridiani shoreline Results in Table 2 are very lower than that in Carr and Head (2003) due to the fact that these authors used a value of 0 for the mean paleoshoreline elevation, whereas we use a mean elevation of –1.5 km following Parker et al. (2000).

Table 2. Basin characteristics at the mean elevations of the proposed Deuteronilus, Arabia and Meridiani shorelines. North polar cap contribution is included in every case.

	Deuteronilus shoreline	**Arabia shoreline**	**Meridiani shoreline**
Mean elevation (km) [a]	−3.792	−2.090	−1.5
Basin area enclosed	2.47	4.66	5.34
Present-day basin volume [b] (10^7 km^3)	1.93	8.66	11.88
Total water volume [c,d] (10^7 km^3)	2.00-2.80	8.77-12.28	11.99-16.79
GEL (km) [c,d]	0.14-0.19	0.61-0.85	0.83-1.16
Mean depth (km) [c,d]	0.81-1.13	1.88-2.63	2.25-3.14
Maximum depth (km) [c]	1.46-2.04	3.16-4.42	3.75-5.25

[a] Mean elevations for Deuteronilus and Arabia shoreline after Carr and Head (2003), and for Meridiani Shoreline after Parker et al. (2000),

[b] North polar cap contribution not included.

[c] Lower limit: present-day topography; Upper limit: water loaded, Airy compensated, topography.

[d] North polar cap contribution included.

These calculations assume that the topography of the northern plains has changed little since the putative shorelines were formed. Irrespective of the accuracy of this assumption, estimations based on observed present-day topography can only provide lower limits to the basins volume. Indeed, the existence of oceans in the northern lowlands would imply that the water column provided an additional load over the lithosphere in the regions covered by water (Leverington et al., 2003; Leverington and Ghent, 2004). The effects of variations of the water load on topography are well known for Earth (for a review see Watts, 2001). Therefore, the weight of the water column would have produced the subsidence of the sea floor during the possible periods in which an ocean occupied the lowlands, increasing the basins volume; the subsequent desiccation of the ocean would results in the opposite effect (Hiesinger and Head, 2000; Thomson and Head, 2001; Kreslavsky and Head, 2002; Leverington et al., 2003; Leverington and Ghent, 2004).

We take into account the effect of water load by assuming Airy compensation to calculate upper limits to the basins volume for Meridiani, Arabia and Deuteronilus shoreline. To assume Airy compensation achieved in the mantle implies that elevation variation in the sea floor due to changes in the height of the overlying water column is

$$\Delta y_{\mathrm{floor}} = \frac{y_{\mathrm{w}} \rho_{\mathrm{w}}}{\rho_{\mathrm{m}}},$$

where y_w is the height of the water column (i.e., the ocean depth), and ρ_w and ρ_m are the ocean and mantle densities, respectively. If y_w is taken as the depth of an ancient ocean, and y is the altitude difference between the ocean basin floor for the empty basin and the sea level when the basin was filled, obviously $\Delta y_{\mathrm{floor}} = y_w - y$, and the isostasy principle requires

$$\frac{y_{\mathrm{w}}}{y} = \frac{\rho_{\mathrm{m}}}{(\rho_{\mathrm{m}} - \rho_{\mathrm{w}})}.$$

So, if y is taken as the present-day depth of the basin under the sea level, then this implies that estimations for the water volume enclosed in the Martian oceans should be increase by a factor y_w/y (with higher ocean density and lower mantle density increasing this factor). If we assume $\rho_w = 1000$ kg m^{-3} and $\rho_m = 3500$ kg m^{-3}, it is obtained $y_w/y = 1.4$. Figure 4 shows basins volume as a function of the elevation level for water loaded, Airy-compensated, topography.

It is important to note that, although water load of putative ancient oceans would result in a substantial increase in the basin volume with respect to calculations based on present-day topography, the assumption of Airy isostasy would imply that the lithosphere has not rigidity, and therefore the increasing factor y_w/y is an upper limit. So, values presented in Table 2 for water volume, GEL (the Global Equivalent Layer if the water is homogeneously distributed on the surface of Mars), mean depth and maximum depth are given as intervals between estimated results for present-day topography and results for water load compensated by Airy isostasy.

In the calculations of total water volumes the north polar cap volume under the appropriate mean shoreline elevation is taken into account (the total volume of the north polar cap is 1.14×10^6 km^3; Smith et al., 2001), since this contributes to the present-day topography. Lithospheric flexure due to north polar cap loading is not considered here, since that the assumption of not flexure represents the lower limit for north polar contribution to the basins volumes, and upper limits are here calculate assuming Airy compensation.

Re-evaluation of Paleoshorelines

The original global mapping of the putative paleoshorelines was limited by resolution of Viking images. Besides this, it is fairly evident that diverse degradational processes could have affected the original morphology (and topography) of any putative paleoshoreline. Thus, reevaluations of paleoshorelines mapping are probably guaranteed. These revaluations would be of great interest to improve the knowledge the hydrogeological history, but also for the tectonothermal history of Mars, because they could affect the elevation range attributed to a given paleoshoreline, and hence the information derived from elevation ranges.

The possibility that the putative Meridiani shoreline could be the same feature as some portions of the Arabia shoreline was first suggested by Ruiz et al. (2003) related to preliminary work about thermal isostasy applied to Mars. Indeed, the mean elevation in the Meridiani shoreline (−1.5 km following Parker et al. (2000)) is roughly similar to that of the Arabia shoreline in northeastern Arabia, Utopia (not taken into account the Isidis impact basin), Elysium, and Amazonis regions. Thus, a possible paleoshoreline might follow the outline of the Arabia shoreline in these regions, but including the outline of Meridiani Shoreline in western Arabia Terra and Sinus Meridiani. The elevation range of this "mixed" Meridiani/Arabia shoreline, although not examined, would be mostly about 2 km, from −1 to −3 km after Ruiz et al. (2004) on the basis of the topography analysis of Arabia shoreline in Carr and Head (2003). This is still far of an equipotential surface, but this Meridiani/Arabia shoreline would be better candidate to represent a paleoequipotential surface than the Arabia shoreline *sensu strito*: for that reason, it was incorporated to the hypothesis for the Martian hydrogeological history suggested by Fairén et al. (2003), in order to represent the boundary of a putative Noachian ocean.

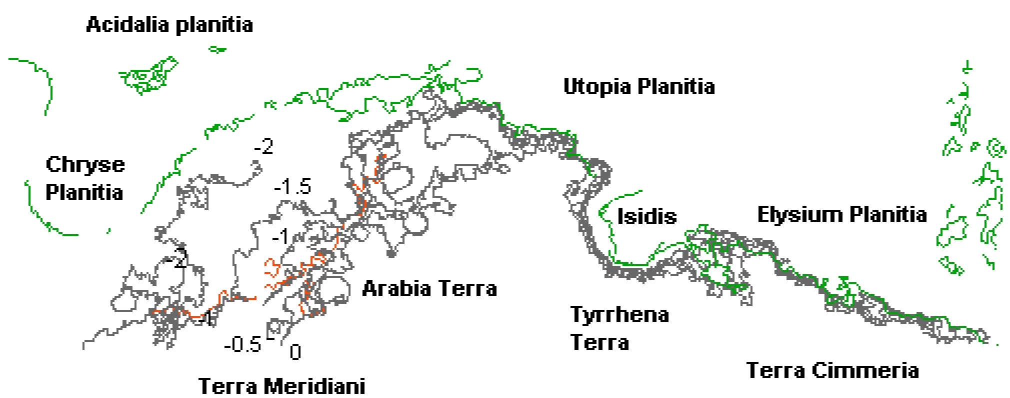

Figure 5. Meridiani (red) and Arabia (green) shorelines, and constant elevation contours in km (black) crossed by the Meridiani shoreline, which are spaced each 0.5 km..

Figure 5 shows Meridiani and Arabia shorelines, as mapped by Clifford and Parker (2001), and constant elevation contours (0.5 km spaced) crossed by the Meridiani shoreline. It can be seen that elevations of the Arabia shoreline at northeastern Arabia, Utopia, and Elysium regions are similar to these along the Meridiani Shoreline, which support the "mixed" Meridiani/Arabia shoreline as a true paleoshoreline. Also is evident that elevations in the Arabia shoreline are much lower in northwestern Arabia Terra, as well as further to the west. Figure 6a shows Meridiani and Arabia shorelines and the contour of the −1.5 km elevation level (the mean level of the Meridiani shoreline after Parker et al. (2000)) superimposed on MOLA topography. The Arabia shoreline at northeastern Arabia, Utopia, Elysium, and Amazonis regions is well close to the −1.5 km elevation level at the majority of places, further supporting the "mixed" Meridiani/Arabia shoreline as a true paleoshoreline. Figure 6b is similar, but showing the contour of the −2.09 kn elevation, corresponding to the mean elevation of the Arabia shoreline *sensu strito*: the Arabia shoreline at Arabia, Utopia, Elysium, and Amazonis regions is at, or generally above, the −2.09 kn elevation level (with the exception of Isidis impact basin, which probably postdates paleoshoreline formation). Thus, the whole topographic range in the Meridiani/Arabia shoreline would be ~1.6 km, between −0.5 and −2.1 km. Moreover, if the Arabia shoreline *sensu strito* is not a true paleoshoreline, then areas, volumes, mean depths and GELs obtained for this "feature" from MOLA topography are not representative of any Martian oceanic stage, but estimations for the −1.5 km elevation level would be roughly appropriate for the Meridiani/Arabia shoreline.

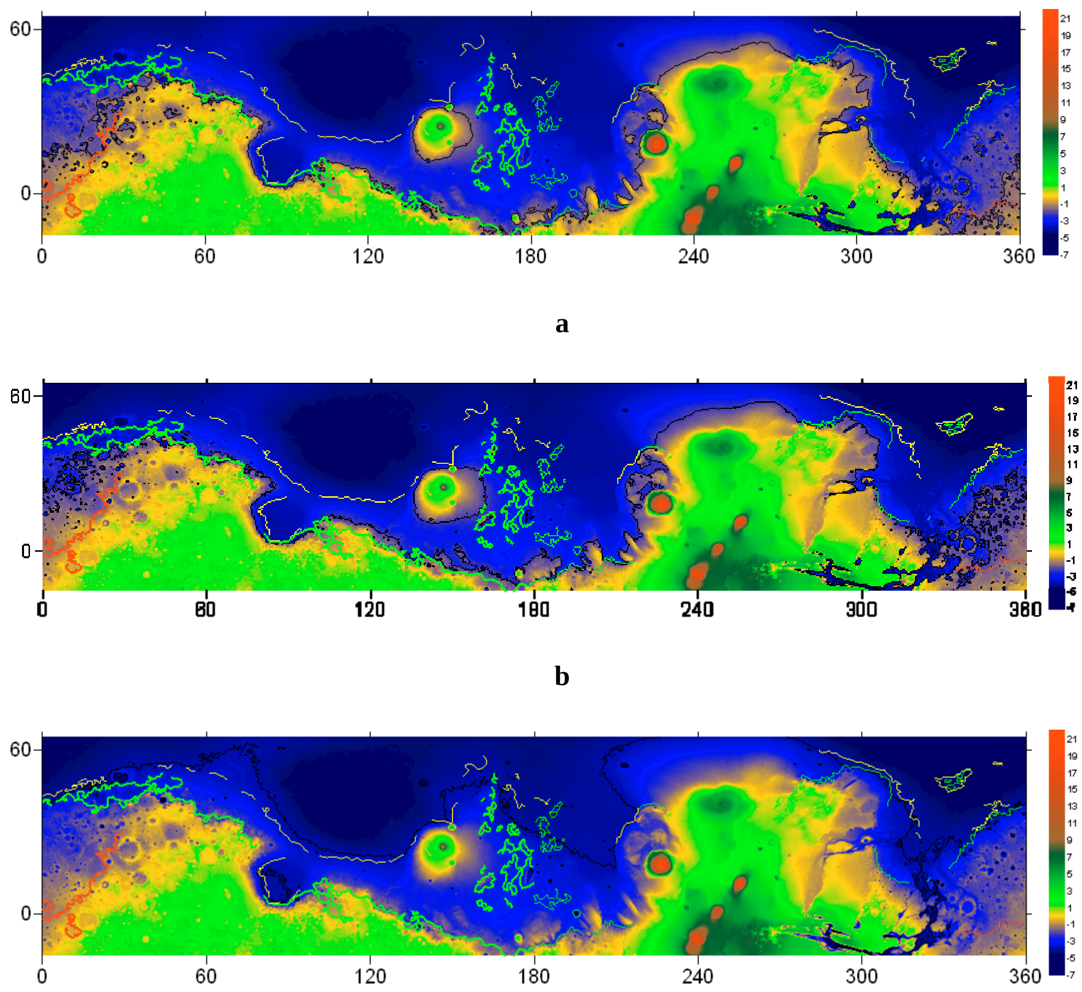

Figure 6. The Deuteronilus (yellow), Arabia (green) and Meridiani (red) shorelines after Clifford and Parker (2001), represented on the Martian topography (scale in km). Also represented (black) are the contour of the (a) -1.5 km, (b) -2.09 km, and (c) -3.792 km elevation levels.

The elevations along putative shorelines on northern Arabia Terra has been recently analyzed in higher resolution (Webb, 2004), finding a elevation of 3707 ± 21 m, for the Arabia shoreline, and two different elevations, 4000 ± 14 m and 4200 ± 12 m, for two separate portions of the Deuteronilus shoreline, which could therefore represent two distinct shorelines. Elevation difference between the two separate portions of the Deuteronilus shoreline is difficultly due to post-formation processes, because elevation in the two portions is nearly constant along distances of about 500 km, and to the clear bimodality in the elevation values. On the other hand, the elevation of the Arabia shoreline in northern Arabia Terra after (Webb, 2004) is intriguingly close to the mean elevation of the Deuteronilus shoreline, and it the possibility of a "mixed" Arabia/Deuteronilus shoreline, which would include the Arabia shoreline in northern Arabia Terra and the Deuteronilus shoreline elsewhere, has been mentioned (Ruiz, 2005).

Figure 6c shows the Arabia and Deuteronilus shorelines, and the contour of the −3.792 km elevation level, the mean elevation of the Deuteronilus shoreline, superimposed on MOLA topography. It is obvious that the Arabia shoreline is very close to −3.792 km elevation level at northwestern Arabia Terra and northeastern Tempe Terra. In turn, Deuteronilus shoreline elevation at Tempe Terra is close to −4 km (see also Carr and Head, 2003), a similar elevation to that found for this feature by Webb (2004) for northern Arabia Terra. Thus, locally at northern Arabia Terra and northeastern Tempe Terra putative shorelines fit well equipotential surfaces, but they are suggesting a complex scenario for the possible evolution of Martian oceans.

Elevation Ranges along Paleoshorelines and Vertical Movements of the Lithosphere

Implications of paleoshoreline reevaluations are evident: the lower the true elevation range of a paleoshoreline the lower the magnitude of vertical movements postdating its formation. For example, elevation range of 1.1 km along the Deuteronilus shoreline is an upper limit, because this range probably includes portions of several different paleoshorelines. Vertical movements deduced from the differences of this feature with respect to an equipotential surface should also be an upper limit.

The fit, although rough, of paleoshorelines to equipotential surfaces would imply a relatively calmed history for the Martian lithosphere, at least since these features were formed. This is clearly the case for the Deuteronilus shoreline *sensu strito*, if this feature is a true paleoshoreline, and moreover for the "revised" Deuteronilus shorelines, which are dating from the Late Hesperian, ~3 Gyr ago (see Table 1). The evidences for a reasonably equipotential Noachian paleoshoreline are attractive, but they must be taken more carefully. If the Meridiani/Arabia shoreline represents a true paleoshoreline, then its whole elevation range of 1.6 km would imply a quite stable lithosphere since 3.5 Gyr ago at least.

By contrast, Gratton et al. (2003) find that the Meridiani, Arabia and Deuteronilus shorelines could fit equipotential surfaces if the reference ellipsoid for the planet has changed with the time, maybe due to the dichotomy formation or Tharsis volcanism. Although this possibility is attractive, it is based on the interpretation of the Meridiani, Arabia, and Deuteronilus *sensu strito* shorelines as true paleoshorelines, which is unlikely (see above).

Thermal isostasy and Thermal Evolution of the Lithosphere

A significant relation exists between Earth's surface elevation and the thermal state of the lithosphere: the warmer the lithosphere, the lower its mean density, and the higher its buoyancy with respect to the underlying fluid materials. This principle (known as thermal isostasy) has been broadly applied to the thermal subsidence of the cooling oceanic lithosphere (e.g., Turcotte and Schubert, 2002), but it can be also applied in a general way to the continental lithosphere (Lachenbruch and Morgan, 1990), including a tectonothermally stable one. This allows the use of topography and surface heat flow data to constrain Earth's continental lithospheric thermal structure (e.g., Tejero and Ruiz, 2002; Lewis et al., 2003). This relation between surface elevation and thermal state of the lithosphere has been also applied to Mars (Ruiz, 2003; Ruiz et al., 2003, 2004).

In this section we present a complete description of the application to Mars of the thermal isostasy concept. We also revise and extend the results obtained about the evolution of the Martian lithosphere.

Thermal Isostasy

Because of thermal expansion and contraction, the elevation of the surface, referenced to the free height of the asthenosphere, depends on the thermal state of the lithosphere and has contributions from the lithospheric mantle and crust,

$$H = H_m + H_c, \tag{1}$$

where H_m and H_c are the lithospheric mantle and crust contribution to the elevation of the surface respectively. (The term lithosphere is used here to define a thermally conductive layer, in which base isostatic compensation can be achieved.) The contribution due to the lithospheric mantle is given by (Lachenbruch and Morgan, 1990)

$$H_m = \alpha(\overline{T}_m - T_a)b_m, \tag{2}$$

where α is the volumetric thermal expansion coefficient, T_a is the temperature of the asthenosphere, $\overline{T}_m$ is the mean temperature of the lithospheric mantle, and b_m is the lithospheric mantle thickness; density differences between asthenospheric and lithospheric mantle are taken as solely due to temperature differences, which is a very reasonable approximation. A similar equation can be written to describe the crustal contribution, but taking into account a correction factor for the lesser crustal density,

$$H_c = \frac{\alpha\rho_c}{\rho_a}(\overline{T}_c - T)b_c, \tag{3}$$

where ρ_c and ρ_a are respectively a reference crustal density and the density of the asthenosphere, and b_c is the crustal thickness. In turn, the mean temperatures of each lithospheric layer is given by

$$\overline{T} = \frac{1}{z_2 - z_1}\int_{z_1}^{z_2} T(z)\mathrm{d}z. \tag{4}$$

where z, z_1 and z_2 are the depth, the depth in the layer top, and the depth at the layer base, respectively. The component of the topography due to thermal isostasy, expressed in terms of heat flow, is (Ruiz, 2003)

$$h = H_m (F_h) + H_c (F_h) - H_m (F_o) - H_c (F_o)\ , \tag{5}$$

where h is the local elevation with respect to a reference elevation, F_h is the local surface heat flow, and F_o is the heat flow for the reference elevation.

Temperature Profiles

Temperature profiles in this chapter are calculated by assuming radioactive heat sources homogeneously distributed in the crust, and linear thermal gradients for the lithospheric mantle mantle. The temperature at a depth z within the crust is given by (Roy et al., 1968)

$$T_z = T_s + \frac{Fz}{k_c} - \frac{Az^2}{2k_c}\ , \tag{6}$$

where T_s is the surface temperature, F is the surface heat flow, k_c is the thermal conductivity of the crust, and A is the volumetric heat production rate. Ruiz (2003) calculate b_m, $\overline{T}_m$, and $\overline{T}_c$ in terms of the surface heat flow, and the proportion f of the heat flow originated from crustal heat sources, assuming that crustal heat sources are homogeneously distributed. The factor f can be formally defined as

$$f = \frac{Ab_c}{F}\ ; \tag{7}$$

so, within the crust, the temperature at a depth z is

$$T_z = T_s + \frac{Fz}{k_c}\left(1 - \frac{fz}{2b_c}\right). \tag{8}$$

The existence of heat sources in the lithospheric mantle is not take into account, because on Earth radiogenic sources are sparse beneath the near-surface radioactive element-rich layer, and within the lithospheric mantle, the heat flow can be assumed constant (e.g., Turcotte and Schubert, 2002); so, within the mantle lithosphere, the temperature at a depth z is

$$T_z = T_c + \frac{F(1-f)(z-b_c)}{k_m}\ , \tag{9}$$

where T_c is the temperature at the crust base, calculated taking $z = b_c$ in equation (8); in turn, b_m is calculated from

$$b_m = b_c + \frac{k_m (T_a - T_c)}{F(1-f)} \quad . \tag{10}$$

Mean lithospheric mantle and crust temperatures are respectively given by

$$\overline{T}_m = \frac{T_a + T_c}{2} \quad , \tag{11}$$

and

$$\overline{T}_c = T_s + \frac{F b_c (1 - f/3)}{2 k_c} \quad . \tag{12}$$

Parameter Values

The calculations have been performed using $\alpha = 3 \times 10^{-5}$ ºC^{-1}, $k_c = 2.5$ W m^{-1} ºC^{-1}, $k_m = 3.5$ W m^{-1} ºC^{-1}, $\rho_c = 2900$ kg m^{-3}, and $\rho_a = 3500$ kg m^{-3} for material properties. The surface temperature is taken as 0ºC, maybe more appropriate for a time in which an ocean is assumed than the current mean surface temperature of about −50ºC (although the results are relatively insensitive to the election of this parameter). The asthenosphere temperature is taken as 1300ºC, which is a value typically used for the Earth's asthenosphere (e.g., Ranalli, 1997). Crustal thickness is assumed to be 40 km, in accordance with the typical mean crustal thickness below the northern lowlands derived from topography and gravity data (Zuber et al., 2000). Two possibilities have been taken for the value of f in equation (8), although we note that this value could locally vary: $f = 0$ (corresponding to a linear thermal gradient through the crust) and $f = 0.5$. The latter value is in accordance with the proposal (made from geochemical arguments drawn from the materials on Mars' surface) that perhaps over 50% (or even 75%) of radioactive heat sources in this planet are placed in its crust (McLennan, 2001, 2003); similarly, in the Earth, the 40-60% of the heat flow lost in continental areas originates from crustal heat sources (Pollack and Chapman, 1977; Turcotte and Schubert, 2002).

Deformation of Paleoshorelines

Ruiz et al. (2004) have used the thermal isostasy concept to show that it is not necessarily true that a paleoequipotential surface implies a good fit to a present-day equipotential surface. A similar conclusion has been obtained taking into account the lithosphere rebound due to water uploading associated to the disappearance of an ocean of irregularly shaped margins (Leverington et al., 2003; Leverington and Ghent, 2004). Here we present the first-order calculations of the magnitude of the relation between possible variations in the thermal state of the lithosphere and elevation differences, which could cause concrete deviations in equipotentiallity along the proposed paleoshorelines. Note that for the purposes of this chapter, only large wavelength topographic differences are relevant, since that the rigidity of the Martian lithosphere could prevent small-scale isostatic adjustment.

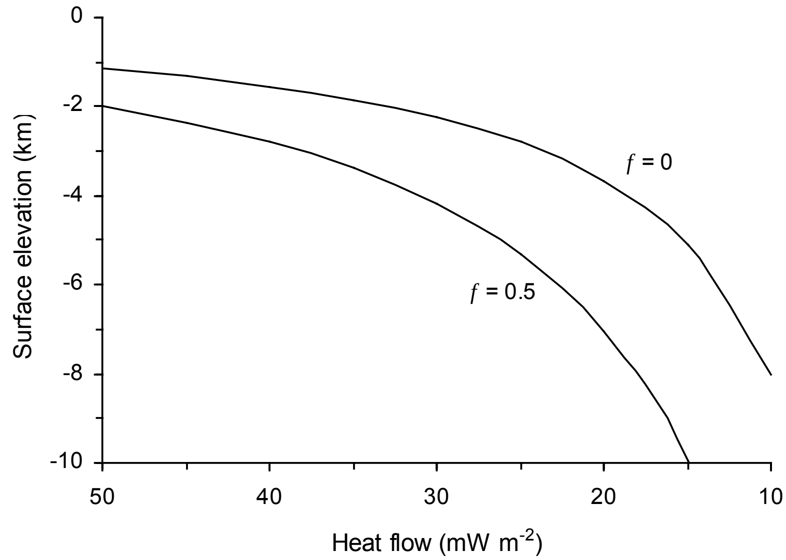

Figure 7. Elevation over the free height of the asthenosphere in terms of surface heat flow for $f = 0$ and $f = 0.5$. Surface heat flow is represented in reverse order (describing the topographic evolution of a cooling region isostatically compensated). Adapted from Ruiz et al. (2004).

Figure 7 shows H in terms of surface heat flow for $f = 0$ and $f = 0.5$. Calculations have been made for a range of F values between 10 and 50 mW m^{-2}, which roughly correspond to the whole range of surface heat flows proposed for diverse regions and times using estimates of the elastic thickness of the lithosphere (McGovern et al., 2002, 2004). It is important to note that the f value can change along a possible paleoshoreline (for example, due to local variations in crustal heat sources, mantle heat flow, or both), or with time (due to waning of radiogenic dissipation intensity or to changes in the efficiency of convective heat transfer). In any case, these possibilities are not important for the purpose of this first-order calculation, which is show the feasibility of differential thermal isostasy histories to affect the large wavelength topography of possible Martian paleoshorelines. For the purposes of this analysis the interesting point is the relative differences of H, and not the absolute values obtained for this parameter (planetary topographies are referred to arbitrary datum). Figure 7 indicate that variations in thermal state of the lithosphere can result in differential thermal isostasy, which in turn can result in important elevation differences, even of kilometric scale as occur on the Earth (Lewis et al., 2003).

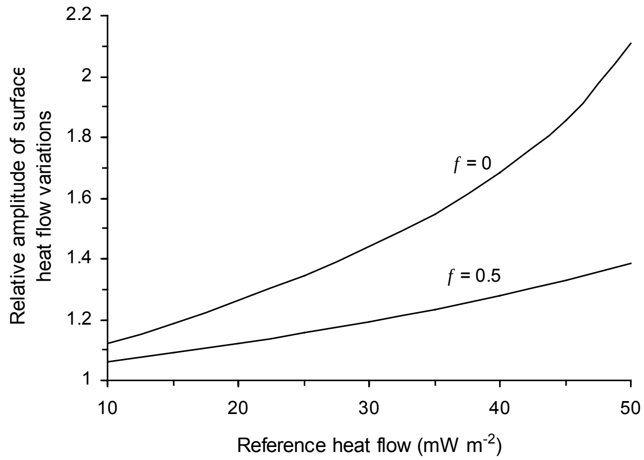

a

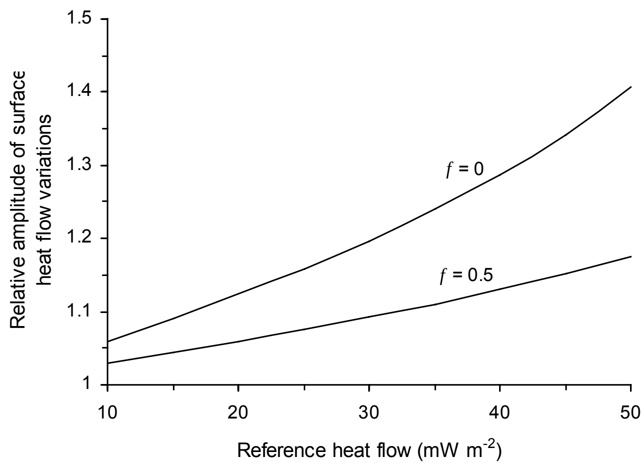

b

Figure 8. Relative amplitude of surface heat flow variations that can produce elevation ranges of 1 (a) and 0.5 (b) km centered on the *H* value corresponding to a reference heat flow in the range from 10 to 50 mW m^{-2}. As in Figure 1 surface heat flow is represented in reverse order. Adapted from Ruiz et al. (2004).

Assuming a Martian paleoshoreline, the posterior attenuation, disappearance (as is expected with the waning of internal heat sources), or formation (if reheating of the lithosphere postdating the shoreline formation occurred) of heat flow variations must result in the deformation of the paleoshoreline topography, deviating it from an equipotential surface. Figure 8 shows the relative amplitude of surface heat flow variations that can produce elevation ranges of 1 and 0.5 km centered on the *H* value corresponding to a reference heat flow in the range from 10 to 50 mW m^{-2}. The relative amplitude of heat flow variations is obtained as the quotient between the maximum and minimum heat flow that can produce positive and negative elevations, respectively, of 0.5 and 0.25 km with respect to the reference *H* value. In Figure 8 it can be seen that ancient surface heat flow variations less than a factor ~2 may account for differences of elevation of 1 km. An elevation range of 0.5 km could be produced by surface heat flow variations less than a factor of ~1.5. These values are further lowered if a substantial amount of the Martian heat sources are located within the crust.

On the Earth, present-day surface heat flow variations expand by more than one order of magnitude (e.g. Pollack et al., 1993). The major part of these variations is due to plate tectonics, but for Mars an early phase of plate tectonics is controversial. Variations in surface heat flow in Earth's continental regions, from contoured maps (Cermak, 1993; Pollack et al., 1993), can be higher than a factor of 2 or 3, sufficient for important deformation of paleoshorelines (see Figure 7). Those areas include terrains of different ages, and it is known for continental areas that an inverse relation exists between surface heat flow and age of the last tectonothermal stabilization (e.g., Hamza, 1979; Vitorello and Pollack, 1980; Cermak, 1993). Moreover, continental heat flow depends also on a wide array of factors, as for example radioactive heat production in the crust, local mantle heat flow, or tectonic or erosive redistribution of crustal heat producing elements (for reviews see Beardsmore and Cull, 2001; Sandiford and McLaren, 2002).

In any case, heat flow variations on old and tectonothermally stable terrestrial continental areas can be as high as a factor ~1.5-2 (e.g., Cermak, 1993; Roy and Rao, 2000; Rolandone et al., 2002). If local variations of surface heat flow of at least similar amplitude existed in Mars during any moment of its history, then these results indicate that differential thermal isostasy should result in important deformation, and deviation of equipotentiallity, along putative shorelines. Moreover, it is significant that if the half of the surface heat flow was originated from crustal heat sources (as it is the case on the Earth) when the paleoshorelines were formed, then heat flow variations lower than a modest factor of ~1.2-1.4 may account for present-day elevation ranges of 0.5-1 km (if, as it seem reasonable, these heat flow variations are currently greatly attenuated). These elevation ranges are respectively similar to the ±1 standard deviation and whole elevation ranges in the Deuteronilus shoreline, but they represent an important amount of deformation along any possible paleoshoreline.

It is important remind that thermal isostasy is only a contributor to the topography. Though it is not our intentions to discuss the many other factors that may have contributed to the modification of an equipotential surface, we highlight that other possibilities may be degradation by wind, water, tectonic, and volcanic modification (e.g., Clifford and Parker, 2001; Fairén et al., 2003), rebound of the lithosphere due to dissipation of a water body (Leverington et al., 2003; Leverington and Ghent, 2004; for a review of isostatic and flexural effects related to changes in sea level see Watts, 2001), flexure (non-thermal) isostasy due to surface loading, erosion, or subsurface magmatic intrusions. In fact, endogenic-driven geologic activity (probably implying vertical movements) and exogenic activity clearly postdates the possible paleoshorelines in Arabia Terra and Tharsis and Elysium (e.g., Head et al., 1999; Anderson et al., 2001). Together, all those possibilities make more pressing the main argument in this section: any paleoequipotential surface dating of the ancient Mars must be importantly deformed at present, even in a range of elevations of a kilometric scale.

Ancient Heat Flow Variations

If the existence of paleoshorelines is accepted, then elevation differences along these paleoshorelines impose constraints to the differences in the evolution of the thermal structure of the lithosphere in shoreline-crossed regions (Ruiz, 2003). Indeed, it is possible to calculate the amplitude of heat flow variations necessary to compensate present-day topography and transform a paleoshoreline into an equipotential surface. If surface heat flow variations on Mars are currently almost disappeared (as it would expectable for an efficiently cooled planet), then the heat flow variations deduced from shoreline topography must be mostly related to the time when this feature was formed. Like other than thermal isostasy processes could have produced vertical movements in the shoreline-crossed regions, the results obtained in this way suppose an upper limit to the amplitude of heat flow variations. Diverse processes, including geomorphologic evolution, can affect small-scale topographic variations, and the rigidity of the Martian lithosphere could also prevent small-scale isostatic adjustment; therefore, large wavelength topographic variations, in which isostatic adjustment can work, are more relevant again for the purposes of this argument.

The calculations have been performed for the Deuteronilus shoreline, but the argument and results are also valid for the outer contact of the Vastitas Borealis Formation (if this is considered to be an ancient oceanic limit) since the ranges of elevations are similar in both features. So, h is taken as ±0.55 km, for a total elevation range of 1.1 km for the Deuteronilus shoreline. This corresponds to a reference elevation (for which $h = 0$ and $F_h = F_o$) of –3.75 km, close to the mean elevation of the Deuteronilus shoreline and to the mean elevation of the termini of the Chryse outflow channels. Like elevation differences along the shoreline must be compensated by heat flow variations, h should have sign minus in equation (5) for mathematical consistency. The F_o value is not known, and for that reason, the calculations have been performed for a range of F_o values between 15 and 35 mW m^{-2}, a range based on estimates (uncertainty included) of the late Hesperian/early Amazonian elastic lithosphere thickness (Zuber et al., 2000; McGovern et al., 2002, 2004).

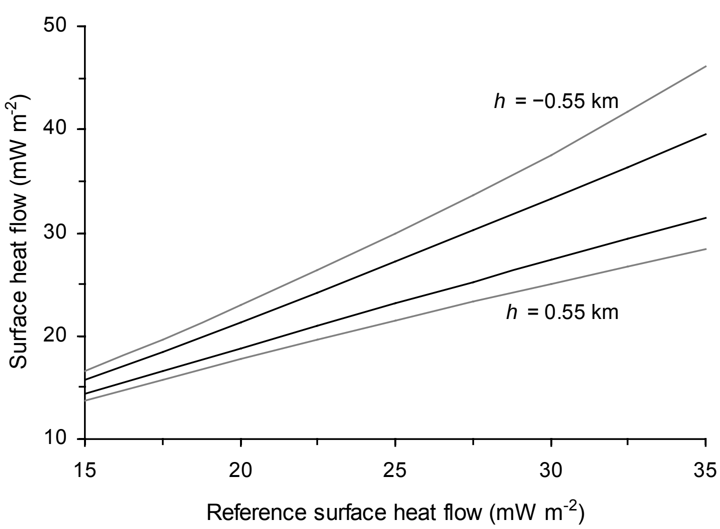

Figure 9. F_h values for h = 550 m (lower curves) and h = –550 m (upper curves) in terms of F_o. Gray and black lines indicate $f = 0$ and $f = 0.5$, respectively. In each case, the difference between the upper and lower curves gives the maximum surface heat flow variations permitted assuming the Deuteronilus shoreline as a paleo-equipotential surface. Adapted from Ruiz (2003).

Figure 9 shows F_h values for h = ±0.55 km in terms of F_o. In each case, the difference between the upper and lower curves gives the maximum heat flow variations allowed, taking into account the Deuteronilus shoreline topography. Figure 10 shows upper limits to the relative amplitude of surface heat flow variations on Deuteronilus shoreline locations; these relative amplitude upper limits are the ratio between the maximum and minimum values shown in Figure 9.

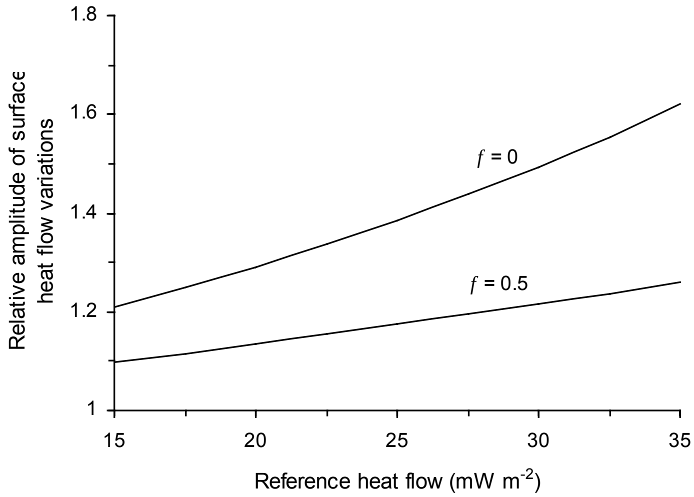

Figure 10. Upper limits to the relative amplitude of surface heat flow variations on the Deuteronilus shoreline locations. These relative amplitude upper limits are given by the ratio between upper and lower values. Adapted from Ruiz (2003).

It can be seen in Figures 9 and 10 that variations in heat flow in regions through the Deuteronilus shoreline were small in the Late Hesperian. In fact, the obtained upper limits for the relative amplitude of these variations are, at most, a factor of 1.6. If crustal heat sources are taken into account, the magnitude of the relative amplitude variations decreases for each given value of F_o. For the F_o range used here, the depth to the 1300ºC isotherm is ~100-300 km for $f = 0$ and ~200-600 km for $f = 0.5$. Since the small radius of Mars the calculations for the case $f = 0.5$ (at low heat flows values) should take in account the spherical shape of Mars. In addition, the range of F_o values used here is based on works assuming linear thermal gradients. Calculation of surface heat flows from elastic thicknesses would result in higher values if heat sources are present in the crust (Solomon and Head, 1990; Ruiz et al., 2005). This, in turn, decreases the depth to the 1300ºC isotherm and also increases the relative amplitude of variations in F_h for the case $f = 0.5$. As the relative amplitude of F_h variations is clearly lower in the $f = 0.5$ case than in the $f = 0$ one, the main conclusions so obtained are not altered.

The upper limits for the relative amplitude of heat flow variations obtained here are clearly lower than those presently observed on Earth. On our planet, the higher heat flows are associated with sea floor spreading centers, but there is not clear evidence for a phase of plate tectonics in the Mars's history (and, in any case, not for the late Hesperian or later on), and so, those very high heat flows are not relevant for the purposed of is chapter. As above mentioned, heat flow show variations in continental areas can be higher than a factor 2-3, and as high as a factor ~1.5-2 in tectonothermally stable terrestrial continental areas. Those areas include terrains of different ages, and it is known for continental areas that an inverse relation exists between surface heat flow and age of the last tectonothermal stabilization (e.g., Hamza, 1979; Vitorello and Pollack, 1980; Cermak, 1993).

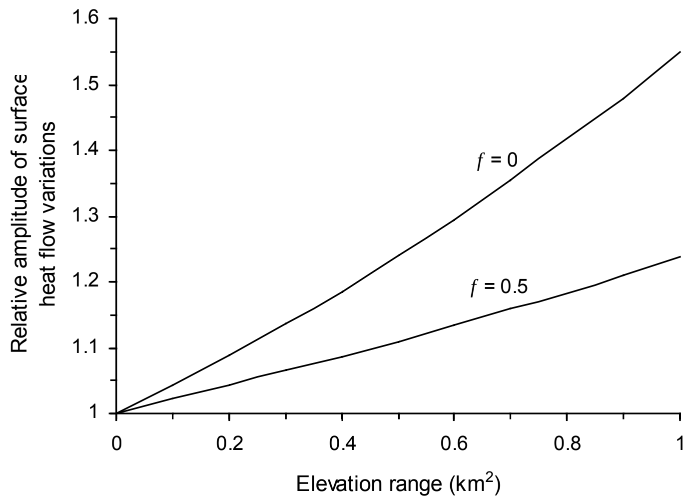

Figure 11. Upper limits to the relative amplitude of surface heat flow variations in terms of the total elevation range of a paleoshoreline, calculated for F_o = 35 mW m^{-2} (the upper limits in the range of heat flows assumed for analyze the Deuteronilus shoreline case) at the H value corresponding to the central value in the elevation range.

If surface heat flow variations on Mars are currently almost disappeared, then the upper limits to the heat flows variations deduced of Deuteronilus shoreline topography are related to the time when this feature was formed (i.e., the Late Hesperian, ~3 Gyr ago; Hartmann and Neukum, 2001). In this case, the present-day elevation range along Deuteronilus shoreline suggests that differences in the thermal state of the lithosphere in the "Deuteronilus shoreline regions" have been relatively small since the feature was formed, and therefore, that very large areas of the Martian lithosphere has been tectonothermally stable since the Late Hesperian. This is consistent with near complete building of the Tharsis rise by the end of the Noachian (Phillips et al., 2001), with a significant decrease in volcanic resurfacing rates following the Hesperian's end (e.g., Hartmann and Neukum, 2001) and with the localization of the waning Amazonian magmatic and tectonic activity at areas in Tharsis and Elysium (e.g., Anderson et al., 2001; Dohm et al., 2001; Head et al., 2001).

Alternatively, reheating of the lithosphere postdating the Deuteronilus shoreline could have caused, or contributed to, the distortion of the topography. In this case, the reheating should have been maintained (at least partially) until the present time, since the dissipation of the thermal anomalies should lead to the disappearance of their effect on the topography. But, as above mentioned, Amazonian geological activity represents the waning and localized magmatic and tectonic activity on Mars, and for that reason, the obtained upper limits to the heat flow variations more probably refer to the thermal state of the Martian lithosphere when the Deuteronilus shoreline was formed.

In summary, if the Deuteronilus shoreline (or equivalently, the outer contact of the Vastitas Borealis Formation) represents a Late Hesperian paleo-equipotential surface, then three conclusions can be deduced from these calculations. First, the relative variations in Late Hesperian surface heat flow in shoreline regions were lower than relative variations in present-day surface heat flow in continental areas on Earth. Second, if substantial amounts of radiogenic heat sources are located in the Martian crust, those relative variations are likely lower. Finally, very large areas of the Martian lithosphere have been tectonothermally stable since (at least) the Late Hesperian.

If the Deuteronilus shoreline is a feature combining portions of several paleoshorelines, then the total elevation range would be lower, and the arguments above more pressing, as clearly illustrated by Figure 11. This figure shows upper limits to the relative amplitude of heat variations, for f = 0 and f = 0.5, as functions of the total elevation range of a paleoshoreline. As only upper limits for a given elevation range are represented, the calculations have been performed for a F_o value of 35 mW m^{-2} (the upper limits in the range of heat flows assumed for analyze the Deuteronilus shoreline case) at the H value corresponding to the central value in the elevation range, and therefore $h = \pm\Delta H/2$.

Conclusion

The range of elevations of the Deuteronilus shoreline is strongly indicating the great tectonothermal stability of the Martian lithosphere since the Late Hesperian, at least. If an important proportion of radioactive heat sources are located in the crust, as geochemical evidences suggest, the lithosphere should have been greatly thermally homogeneus in "Deuteronilus shoreline" regions when coastal processes creating this paleoshoreline were working.

There are evidences suggesting that the lateral continuity of the originally proposed paleoshorelines is not well established: diverse division and mixing of the originally proposed paleoshorelines seem be required. These revaluations are of great interest for the understanding of the evolution of the Martian lithosphere, because they would modify the elevation range attributed to a given paleoshoreline. Thus, it is necessary a careful geomorphologic reassessment of the diverse features interpreted as paleoshorelines and of the relation among them. The Deuteronilus shoreline (*sensu strito*) seems integrate portions of several separate paleoshorelines, which would imply a still higher thermal stability and homogeneity of the lithosphere by the latest ~3 Gyr. The confirmation of the Meridiani/Arabia shoreline would be indicative of a longer lithospheric stability.

Acknowledgments

The authors thank Frank Columbus for your invitation to prepare this chapter. JR was supported by a grant of the Spanish Secretaría de Estado de Educación y Universidades.

References

[1] Anderson, S.; Grimm, R. E. *J. Geophys. Res.* 1998, 103, 11,113-11,124.

[2] Anderson, R. C.; Dohm, J. M.; Golombek, M. P.; Haldemann, A. F. C.; Franklin, B. J.; Tanaka, K. L.; Lias, J.; Peer, B. *J. Geophys. Res.* 2001, 106, 20,563-20,585.

[3] Beardsmore, G. R.; Cull, J. P. *Crustal Heat Flow. A Guide to Measurement and Modelling*; University Press: Cambridge, UK, 2001; pp 1-324.

[4] Breuer, D.; Spohn, T. *J. Geophys. Res.* 2003, 108 (E7), 8.1-8.13.

[5] Carr, M. H.; Head, J.W. *J. Geophys. Res.* 2003, 108 (E5), 8.1-8.28.

[6] Cermak, V. *Phys. Earth Planet. Inter.*1993, 79, 179-193.

[7] Choblet, G.; Sotin, C. *Geophys. Res. Lett.* 2001, 28, 3035-3038.

[8] Clifford, S. M.; Parker, T. J. *Icarus* 2001, 154, 40–79.

[9] Comer, R. P.; Solomon, S. C.; Head, J. W. *Rev. Geophys.* 1985, 23, 61-92.

[10] Dohm, J. M.; Ferris, J. C.; Baker, V. R.; Anderson, R. C.; Hare, T. M.; Strom R. G.; Barlow N. G.; Tanaka, K. L.; Klemaszewski, J. E.; Scott D. H. *J. Geophys. Res*. 2001, 106, 32,943-32,958.

[11] Edgett, K. S.; Parker, T. J. *Geophys. Res. Lett.* 1997, 24, 2897-2900.

[12] Fairén, A. G.; Dohm, J. M., Baker V. R.; de Pablo M. A.; Ruiz J.; Ferris J. C.; Anderson, R. C. *Icarus* 2003, 165, 53-67, 2003.

[13] Grasset, O.; Parmentier, E. M. *J. Geophys. Res.* 1998, 103, 18,171-18.181.

[14] Gratton, R.; Mareschal, J.; Sotin, C. *Eos Trans. AGU Fall Meet. Suppl.* 2003, 84(46), abstract G41B-0033.

[15] Hamza, V. M. *Pure Appl. Geophys.* 1979, 117, 65-74.

[16] Hartmann, W. K. *Icarus* 2005, 174, 294-320.

[17] Hartmann, W. K.; Neukum, G. *Space Sci. Rev.* 2001, 96, 165-194.

[18] Hauck, S. A.; Phillips, R. J. *J. Geophys. Res.* 2002, 107 (E7), 6.1-6.19.

[19] Head, J. W.; Kreslavsky, M.; Hiesinger, H.; Ivanov, M. A.; Pratt, S.; Seibert, N.; Smith, D. E.; Zuber, M. T. *Geophys. Res. Lett.* 1998, 25, 4401-4404.

[20] Head, J. W.; Hiesinger, H.; Ivanov, M. A.; Kreslavsky, M. A.; Pratt, S.; Thomson, B. J. *Science* 1999, 286, 2134-2137.

[21] Head, J. W.; Greeley R.; Golombek, M. P.; Hartmann, W. K.; Hauer, E.; Jaumann, R.; Masson, P.; Neukum, G.; Nyquist, L. E.; Carr, M. H. *Space Sci. Rev.* 2001, 96, 263-292.

[22] Head, J. W.; Kreslavsky, M. A.; Pratt, S. *J. Geophys. Res.* 2002, 106 (E1), 3.1-3.29.

[23] Hiesinger, H.; Head, J. W. *J. Geophys. Res.* 2000, 105, 11,999-12,022.

[24] Ivanov, M. A.; Head, J. W. *J. Geophys. Res.*, *106*, 3275-3295, 2001.

[25] Kiefer, W. S. *Earth Planet. Sci. Lett.* 2004, 222, 349-361.

[26] Kreslavsky, M. A.; Head, J. W. *J. Geophys. Res.* 2002, 107 (E12), 4.1-4.25.

[27] Lachenbruch, A. H.; Morgan, P. *Tectonophysics* 1990, 174, 39–62.

[28] Leverington, D. W.; Ghent R. R. *J. Geophys. Res.* 2004, 109 (E01005), 1-10.

[29] Leverington, D. W.; Ghent, R. R.; Irwin R. P.; Craddock R. A.; Maxwell T. A. *Lunar Planet. Sci.* 2003, 34, abstract 1282.

[30] Lewis, T. J.; Hyndman, R. D.; Flück P. *J. Geophys. Res.* 2003, 108 (B6), 16.1-16.18.

[31] Malin, M. C.; Edgett, K.C. *Geophys. Res. Lett.* 1999, 26, 3049-3052.

[32] Malin, M. C.; Edgett, K.C. *J. Geophys. Res.* 2001, 106, 23,429-23,570.

[33] McGovern, P. J.; Solomon, S. C.; Smith, D. E.; Zuber, M. T.; Simons, M.; Wieczorek, M. A.; Phillips, R. J.; Neumann, G. A.; Aharonson, O.; Head, J. W. *J. Geophys. Res.* 2002, 107 (E12), 19.1-19.25.
[34] McGovern, P. J.; Solomon, S. C.; Smith, D. E.; Zuber, M. T.; Simons, M.; Wieczorek, M. A.; Phillips, R. J.; Neumann, G. A.; Aharonson, O.; Head, J. W. *J. Geophys. Res.* 2004, 109 (E07007), 1-5.
[35] McKenzie, D.; Barnett, D. N.; Yuan, D. L. *Earth Planet. Sci. Lett.* 2002, 195, 1-16.
[36] McLennan, S. M. *Geophys. Res. Lett.* 2001, 28, 4019-4022.
[37] McLennan, S. M. *Sixth International Conference on Mars* 2003, abstract 3099.
[38] Nimmo, F.; *J. Geophys. Res.* 2002, 107 (E11), 27.1-27.16.
[39] Nimmo, F.; Stevenson, D. J. *J. Geophys. Res.* 2000, 105, 11,969-11.979.
[40] Öner, A. T.; Ruiz, J.; Fairén, A. G.; Tejero, R.; Dohm J. M. *Lunar Planet. Sci.* 2004, 35, abstract 1319.
[41] Parker, T. J.; Saunder, R. S.; Schneeberger, D. M. *Icarus* 1989, 82, 111-145.
[42] Parker, T. J.; Gorsline, D. S.: Saunders, R. S.; Pieri, D. C.; Schneeberger, D. M. *J. Geophys. Res.* 1993, 98, 11,061-11,078.
[43] Parker, T. J.; Clifford, S. M.; Banerdt, W. B. *Lunar Planet. Sci.* 2000, 31, abstract 2033.
[44] Parker, T. J.; Grant, J. A.; Franklin B. J.; Rice J. W. *Lunar Planet. Sci.* 2001, 32, abstract 2051.
[45] Phillips R. J. et al. *Science* 2001, 291, 2587-2591.
[46] Pollack, H. N.; Chapman, D. S. *Earth Planet. Sci. Lett.* 1977, 34, 174-184.
[47] Pollack, H. N.; Hunter, S. J.; Johnson, J. R. *Rev. Geophys.* 1993, 31, 267-280.
[48] Ranalli, G., *Geol. Soc. Spec. Publ.* 1997, 121, 19-37.
[49] Rolandone, F.; Jaupart, C.; Mareschal, J. C.; Gariépy, C.; Bienfait, G.; Carbonne, C., Lapointe, R. *J. Geophys. Res.* 2002, 107 (B12), 7.1-7.19.
[50] Roy, R. F.; Blackwell, D. D.; Birch, F. *Earth Planet. Sci. Lett.* 1968, 5, 1-12.
[51] Roy, S.; Rao, R. U. M. *J. Geophys. Res.* 2000, 105, 25,587-25,604.
[52] Ruiz, J. *J. Geophys. Res.* 2003, 108 (E11), 8.1-8.5.
[53] Ruiz, J. *Lunar Planet. Sci.* 2005, 36, abstract 1135.
[54] Ruiz, J.; Fairén, A. G.; de Pablo, M. A. *Lunar Planet. Sci.* 2003, 34, abstract 1090.
[55] Ruiz, J.; Fairén, A. G.; Dohm, J. M.; Tejero, R. *Planet. Space Sci.* 2004, 52, 1297-1301.
[56] Ruiz, J.; McGovern, P. J.; Tejero, R. *Earth Planet. Sci. Lett.* 2006, 241, 2-10.
[57] Salamuniccar, G. *Lunar Planet. Sci.* 2004, 35, abstract 1992.
[58] Sandiford, M.; McLaren, S. *Earth Planet. Sci. Lett.* 2002, 204, 133-150.
[59] Schultz, R. A.; Lin, J. *J. Geophys. Res.* 2001, 106, 16,549-16,566.
[60] Schultz, R. A.; Watters, T. R. *Geophys. Res. Lett.* 2001, 28, 4659-4662.
[61] Solomon, S. C.; Head, J. W. J. Geophys. Res. 1990, 95, 11,073-11,083.
[62] Schubert, G.; Spohn, T. *J. Geophys. Res.* 1990, 95, 14,095-14,104.
[63] Schubert, G.; Solomon, S. C., Turcotte, D. L.; Drake, M. J., Sleep, N. H. In *Mars*; Kieffer H.; Jakosky, B. M.; Snyder, C. W.; Matthews, M. S.; Eds.; University of Arizona Press: Tucson, AZ, 1992; pp 249-297.
[64] Smith, D. E. et al. *Science* 1999, 284, 1495-1503.
[65] Smith, D. E. et al. *J. Geophys. Res.* 2001, 106, 23,689-23,722.
[66] Spohn, T.; Acuña, M. H.; Breuer, D.; Golombek, M.; Greeley, R., Halliday, A.; Hauber, E.; Jaumann, R.; Sohl, F. *Space Sci. Rev.* 2001, 96, 231-262.
[67] Squyres, S. W. et al. *Science* 2004, 306, 1709-1714.

[68] Stevenson, D. J.; Spohn, T.; Schubert, G. *Icarus* 1983, 54, 466-489.
[69] Tanaka, K. N.; Scott, D.H.; Greeley, R. 1992. In *Mars*; Kieffer H.; Jakosky, B. M.; Snyder, C. W.; Matthews, M. S.; Eds.; University of Arizona Press: Tucson, AZ, 1992; pp 345-383
[70] Tejero, R.; Ruiz, J. *Tectonophysics* 2002, 350, 49-62.
[71] Thomson, B. J.; Head, J. W. *J. Geophys. Res.* 2001, 106, 23,209-23,230.
[72] Turcotte, D. L.; Schubert, G. *Geodynamics. Second edition*; Cambridge University Press: Cambridge, UK, 2002; pp 1-456.
[73] Vidal, A.; Mueller, K. M.; Golombek, M. P. *Lunar Planet. Sci.* 2005, 36, abstract 2333.
[74] Vitorello, I.; Pollack, H. N. *J. Geophys. Res.* 1980, 85, 983-995.
[75] Watts, A. B. *Isostasy and flexure of the lithosphere*; Cambridge University Press: Cambridge, UK, 2001; pp 1-458.
[76] Webb, V. E. *J. Geophys. Res.* 2004, 109 (E09010), 1-12.
[77] Webb, V. E.; McGill, G. E. *Lunar Planet. Sci.* 2003, 34, abstract 1132.
[78] Zuber, M. T. et al. *Science* 2000, 287, 1788-1793.